# Absolute Rate Constants of $Cr_2$ ($X\ ^1\Sigma_g{}^+$) with $O_2$, $NH_3$, and $C_2H_4$ in the Gas Phase at Room Temperature

**Yo-ichi Ishikawa,* Hiroshi Ogawa, and Takayuki Iwaki**

Department of Chemistry and Materials Technology, Kyoto Institute of Technology, Matsugasaki, Sakyo-ku,
Kyoto 606-8585

(Received September 25, 2001)

The gas-phase reactivities of ground-state chromium dimers ($Cr_2$ ($X\ ^1\Sigma_g{}^+$)) for three small molecules ($O_2$, $NH_3$, and $C_2H_4$) were investigated in a mass-flow controlled cell. The transient concentration of $Cr_2$ ($X\ ^1\Sigma_g{}^+$, $v = 0$) produced by pulsed 266-nm laser photolysis of $[Cr(CO)_6]$ was monitored by a time-resolved laser-induced fluorescence (LIF) at 459.67 nm ($A\ ^1\Sigma_u{}^+$, $v'' = 0 \leftarrow X\ ^1\Sigma_g{}^+$, $v' = 0$). The *pseudo*-first-order decay rates of $Cr_2$ ($X\ ^1\Sigma_g{}^+$) were observed to increase linearly with increasing $O_2$ and $NH_3$ pressure, giving *pseudo*-second-order rate constants of $(2.3 \pm 0.3)\times10^{-11}$ $cm^3$ $molecule^{-1}$ $s^{-1}$ for $Cr_2 + O_2$ and $(4.3 \pm 0.8)\times10^{-13}$ $cm^3$ $molecule^{-1}$ $s^{-1}$ for $Cr_2 + NH_3$ under 6.0-Torr total pressure with Ar buffer gas at room temperature. On the other hand, $C_2H_4$ was apparently found not to react with $Cr_2$ ($X\ ^1\Sigma_g{}^+$) under our experimental conditions. In the $Cr_2 + O_2$ reaction, the *pseudo*-second-order rate constants were found to depend on the total pressure, and the limiting low-pressure rate constant was estimated to be $(5.9 \pm 2.5)\times10^{-28}$ $cm^6$ $molecule^{-2}$ $s^{-1}$.

The interaction between the transition-metal centers and small molecules plays an important role in numerous fields of chemistry, physics, and biology. To elucidate these interactions, transition-metal chemistry in the gas phase has been extensively studied for the last several decades, where the "pure" reactivity of the "naked" metal center could be observed free from interruption of environmental chemical species.[1–6] Such studies have the potential to prove simple models for the intricate interaction between active sites on transition metals and small molecules. A rich and varied chemistry involving transition-metal centers has also attracted the attention of theorists, besides experimentalists.[7,8]

Both structural and spectroscopic information on transition-metal dimers has recently been acquired.[9,10] On the contrary, relatively little is known about the detail reactivity of transition-metal dimers with small molecules. This might be due to the less reactivity of metal dimers observed in cluster-beam experiments, probably because of their large stabilization originating in multiple bonds.[11–14] Some absolute rate constants of neutral-metal dimers, such as $Cu_2$,[15,16] $Ag_2$,[16] $Au_2$,[16] and $Mo_2$,[17] with small molecules have been measured using by a recent experimental setup with a laser vaporization/fast-flow reactor/LIF developed by L. Lian et al. They have reported the experimental fact that there is a large difference in the chemical reactivity between Mo atoms and $Mo_2$ dimers, where Mo can react with a π-acceptor, such as $C_2H_4$, but not with a σ-donor, such as $NH_3$, while $Mo_2$ has a counter reactivity. In these metal dimers, the reaction of $M_2$ with a ligand L was found to form an association product of $[M_2\text{-}L]$. One of the most important information is whether or not the chemical-bond activation of a ligand occurs in the association process. Though there seems to be no clear answer to this question so far, the accumulation of experimental data concerning the metal dimer reactivity with small ligands will be useful to elucidate this problem in cooperation with quantum chemistry.[7, 8, 18–20]

A multiphoton dissociation (MPD) of $[Mo(CO)_6]$ has been reported to produce $Mo_2$ effectively, other than Mo atoms, in a UV-vis emission study.[21, 22] The MPD of $[M(CO)_6]$ seems to be a more convenient technique for the pulse production of $M_2$ metal dimers compared to laser vaporization, because it is experimentally simple and gives a homogeneous distribution of $M_2$. Moreover, this technique is expected to give an absolute reaction rate constant for neutral metal dimers, because the absolute pressure of the reactant can be more precisely and easily controlled in a nearly static cell. In this study, we examined the reactivity of the chromium dimer, $Cr_2$, with small molecules of $O_2$, $C_2H_4$, and $NH_3$ in the gas phase by applying a 266-nm MPD of $[Cr(CO)_6]$ to the pulse production of the chromium metal dimer.

## Experimental

A 266-nm multiphoton decomposition of $[Cr(CO)_6]$ (ca. 10 mTorr) was applied for the pulse production of $Cr_2$ ($X\ ^1\Sigma_g{}^+$) or Cr ($a\ ^7S_3$). $[Cr(CO)_6]$ (Aldrich, 99%) was degassed by several freeze-thaw cycles at −10 °C and used without further purification. The sample mixture ($[Cr(CO)_6]$/Ar (as a carrier and buffer gas)/a reactant gas ($O_2$, $C_2H_4$, or $NH_3$)) flowed slowly through a glass cell with two suprasil windows. The flow quantity of each gas was controlled by a calibrated mass-flow controller (STEC-400MARK2 or 3: full scale, 10 sccm; accuracy, < ±0.2 sccm) prior to admission to the reaction cell. The mass-flow controller was used as purchased without further calibration. The total flow rates were between 5–10 sccm and the reactant ($O_2$, $C_2H_4$, or $NH_3$) flow rate was 0.02–1.0 sccm. The total pressures and the partial pressure of the reactant in the flow cell were monitored with a capacitance manometer (MKS 220BH; full scale, 10 Torr; accuracy,

$< \pm 0.015$ Torr) attached directly to the center of the flow cell. Ar (Sumitomo Seika, $> 99.999\%$), $O_2$ (Sumitomo Seika, $> 99.8\%$), $NH_3$ (Sumitomo Seika, $> 99.99\%$), and $C_2H_4$ (Takachiho, $> 99.9$ %) were used as purchased.

The transient concentration of the chromium metal species ($Cr_2$ (X $^1\Sigma_g{}^+$) or Cr (a $^7S_3$)) was monitored in the reaction cell using a time-resolved laser-induced fluorescence (LIF) technique[23, 24] at room temperature ($300 \pm 3$ K). The photolysis UV source was a pulsed Nd:YAG laser (Spectron SL803; $\lambda = 266$ nm). The 266-nm laser beam was focused at the center of the reaction cell using a quartz lens ($f = 15$ cm) to induce the MPD of [Cr(CO)$_6$]. A monitoring source for time-resolved LIF detection was a Nd:YAG laser (Spectra-Physics GCR290-10) pumped OPO laser (Spectra-Physics MOPO-730, line width $\cong 0.4$ cm$^{-1}$), which was used with 10 Hz repetition rate synchronized with the photolysis light by using a digital delay generator (SRS DG535). The two laser beams were arranged to be collinear and counter-propagating. The linear dependence of the LIF intensity on the monitoring laser intensity was experimentally ascertained before each measurement, and the LIF signal intensity was corrected for the intensity pulse-to-pulse fluctuation of the monitoring laser. The raw output signals from the photomultiplier (Hamamatsu R-928) set behind an exit slit of a Spex Minimate monochromator (20 cm in focal length; $\Delta\lambda \sim 20$ nm with 5-mm slit) were first amplified by means of a PAR model 115 preamplifier. The amplified signal was then treated with a digital oscilloscope (Tektronix TDS320) for time-resolved measurements, and the digitized output was stored and analyzed by a personal computer, or with a gated boxcar averaging module (EG&G PAR model 162/165) for spectrum measurements. The aperture duration ($\tau_g$) and the time constant ($\tau_c$) used for the boxcar averager were 100 ns and 10–100 µs (each point averaged over 10–100 laser shots), respectively.

## Results and Discussion

**Formation of $Cr_2$ (X $^1\Sigma_g{}^+$) in UV-MPD of [Cr(CO)$_6$]. a. Time-Evolution of LIF Spectra of $Cr_2$ (X $^1\Sigma_g{}^+$).** The time-evolution of the LIF spectra of $Cr_2$ (A $^1\Sigma_u{}^+ \leftarrow$ X $^1\Sigma_g{}^+$), following the 266-nm pulse photolysis of [Cr(CO)$_6$], are shown in Fig. 1, which is very similar to the absorption spectra of $Cr_2$(X) formed in the laser vaporization of chromium metal.[25–27] Two sharp transition lines with signs of A1 and A2 were assigned to chromium atom transitions (A1; y $^5P_2 \leftarrow$ a $^5D_1$, 459.27 nm: A2; y $^5P_3 \leftarrow$ a $^5D_3$, 460.20 nm).[28] A systematic modulation with $J$ seen in the rotational structure has been interpreted in terms of a two-step predissociation of the A state.[25] Because the line width of the LIF spectra was restricted by that of the monitoring laser ($\Delta\bar{\nu} \sim 0.4$ cm$^{-1}$), the rotational structure ($\overline{B} \sim 0.2298$ cm$^{-1}$) could not be completely resolved. Thermal equilibrium was considered to be established within 1 µs in the rotational mode from the resemblance of the intensity ratio between the modulated four bands at ~459.48, ~459.67, ~459.85, and ~460.07 nm after 5 µs within our experimental scatter. In the $Mo_2$ measurement, where $Mo_2$ was produced by MPD of Mo(CO)$_6$ under a similar condition to this experiment, the spectrum simulation showed that the rotational population was thermally equilibrated within 1 µs, and that the quantity of the vibrationally excited $Mo_2$ was estimated to be less than 20%.[24] Thus, the rotation-vibration relaxation was not taken into consideration in the kinetic analysis. $C_2H_4$ addition is shown not to affect the decay behavior of $Cr_2$ in the result section. A polyatomic molecule, such as $C_2H_4$, can be expected to be effective in the vibrational relaxation of $Cr_2$. The above fact that $C_2H_4$ addition has only a small influence on the decay behavior also supports the idea that vibrational relaxation processes can be ignored in a kinetic analysis.

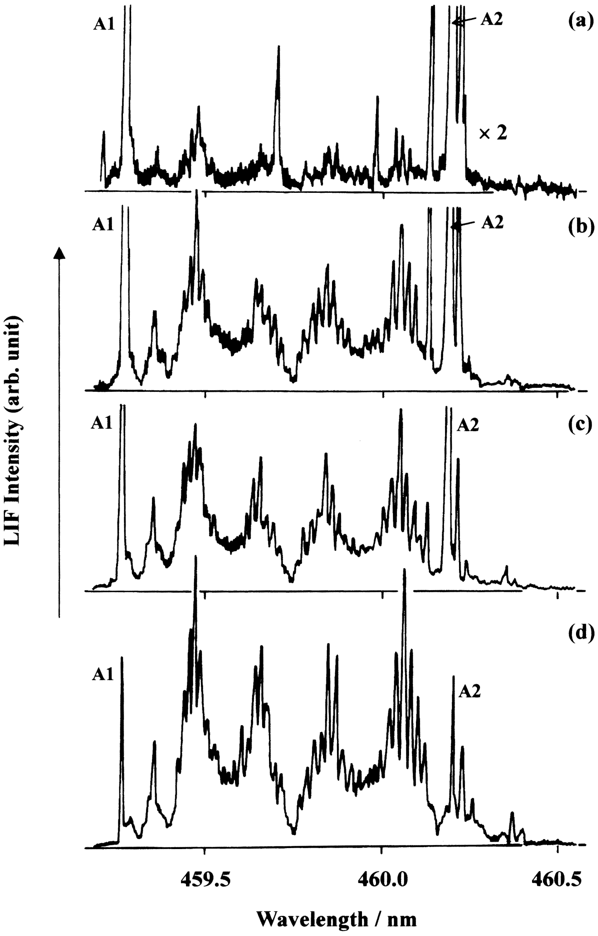

Fig. 1. Time evolution of LIF spectra following the 266-nm multiphoton decomposition of [Cr(CO)$_6$] (ca. 10 mTorr) at 6.0 Torr total pressure with Ar buffer. The spectra were observed at 1 (a), 5 (b), 10 (c), and 40 µs (d) after photolysis laser pulse. Two sharp intense absorptions are assigned to Cr atom transitions (A1; y $^5P_2 \leftarrow$ a $^5D_1$, 459.27 nm: A2; y $^5P_3 \leftarrow$ a $^5D_3$, 460.20 nm). Laser fluence at focus was estimated to be about 0.3 J cm$^{-2}$. Spectrtal resolution was about 0.3 cm$^{-1}$.

**b. Time-Resolved Production Figures of $Cr_2$ (X $^1\Sigma_g{}^+$).** Figure 2 shows typical production time features of $Cr_2$ (X $^1\Sigma_g{}^+$, $v = 0$; monitored at 459.67 nm) together with Cr (a $^7S_3$; monitored at 429.00 nm) as a reference. There is a large difference in the production figures in this time region ($< 1$ µs) between Cr and $Cr_2$. The production curve of Cr atoms has a fast rise within 10 ns, and a gradual increase, while the production curve of $Cr_2$ dimers has only a gradual increase. However, this is not surprising because Cr atoms can be produced in the primary multiphoton dissociation of [Cr(CO)$_6$], but the formation of the $Cr_2$ dimer requires some secondary bimolecular reactions involving at least two Cr atoms. An emission study of the multiphoton dissociation of [Mo(CO)$_6$] has shown that "early"

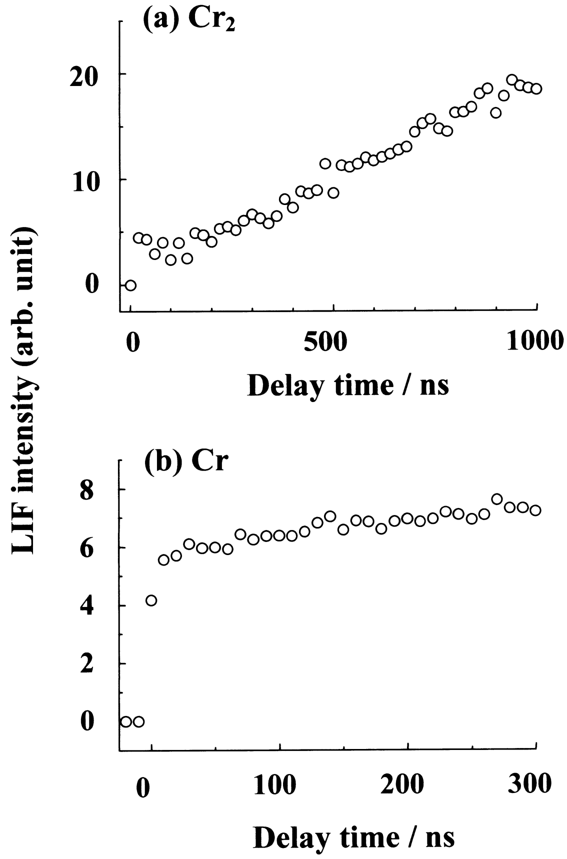

Fig. 2. Typical production time profiles of $Cr_2$ (X $^1\Sigma_g{}^+$) (a: monitored at 459.67 nm (A $^1\Sigma_g{}^+ \leftarrow$ X $^1\Sigma_g{}^+$)) and Cr (a $^7S_3$) (b: monitored at 429.00 nm (z $^7P_2 \leftarrow$ a $^7S_3$)) following the 266-nm multiphoton decomposition of $[Cr(CO)_6]$ (ca. 10 mTorr) at 6.0 Torr total pressure with balance Ar.

production of emissive Mo* atoms with a similar time profile to the photolysis pulse can be attributed mainly to the photodissociation process, while "late" production is mainly due to a neutralization processes of ionic species.[29]

Under the experimental conditions, a rise in the $Cr_2$ concentration could be seen in the time region until 20 µs. When there was no reactant, except for $Cr(CO)_6$ and Ar, the first-order decay rate of $Cr_2$ (X $^1\Sigma_g{}^+$) was observed to be about $5\times10^3$ $s^{-1}$. The decay rates were found to decrease as the total pressure increased by a further addition of Ar in the region of 2–9 Torr (1 Torr ≈ 133.322 Pa), suggesting that the decay was mainly due to the diffusion of $Cr_2$ from the observation zone.

**Addition Effects of Simple Molecules on $Cr_2$ (X $^1\Sigma_g{}^+$) Kinetics.** The decay rates of $Cr_2$ (X $^1\Sigma_g{}^+$, $v = 0$) as a function of the additive pressure were ordinarily measured at 6.0-Torr total pressure with balance Ar. The concentration of $Cr_2$ was monitored at 459.64 nm (A $^1\Sigma_u{}^+$, $v' = 0 \leftarrow$ X $^1\Sigma_g{}^+$, $v'' = 0$, $J'' \approx 8$) following the 266-nm multiphoton decomposition of $[Cr(CO)_6]$ in both the absence and presence of the reactant. During the course of doing this measurement, the reaction rate constants of Cr (a $^7S_3$) at 429.00 nm (z $^7P_2 \leftarrow$ a $^7S_3$) were also reinvestigated in order to check our experimental technique. The error shown in the kinetic constant means one standard deviation ($\pm\sigma$) in the least-squares fitting.

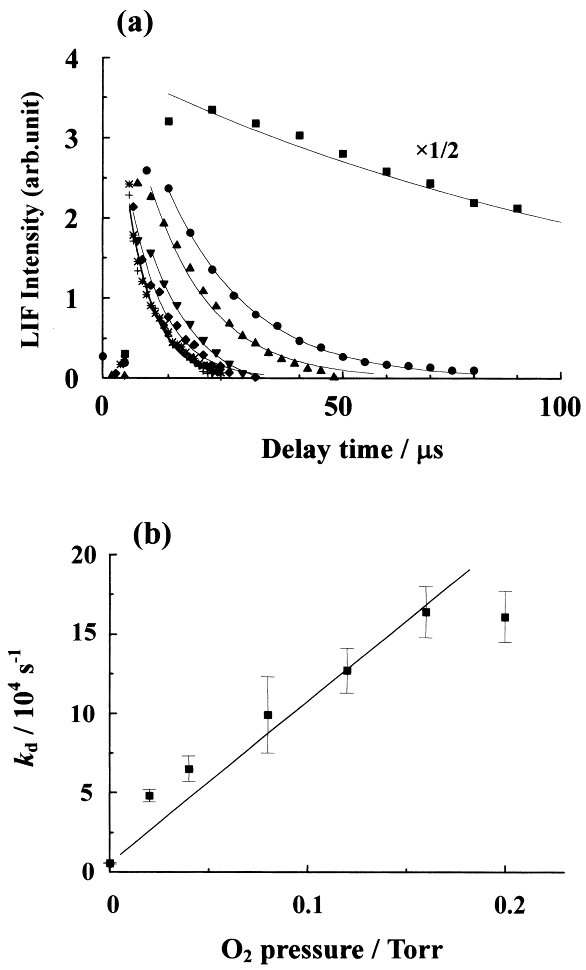

Fig. 3. (a) $O_2$ addition effects on the transient LIF curves of $Cr_2$ (X $^1\Sigma_g{}^+$). $O_2$ pressures are 0.0 (■), 0.02 (●), 0.04 (▲), 0.08 (▼), 0.12 (◆), 0.16 (+), and 0.20 Torr (*); Each solid line is a single-exponential decay fit obtained with an appropriated decay rate. (b) Determination of the *pseudo*-second-order rate constants ($k^{(2)}$); Solid line is a linear fit.

**a. $O_2$ Addition.** Figure 3 shows the $O_2$ addition effects on the transient LIF curves of $Cr_2$ (X $^1\Sigma_g{}^+$) at 6.0 Torr total pressure with balance Ar. $O_2$ addition apparently makes the decay of $Cr_2$(X) faster. It is noteworthy that there was a significant decrease in the dimer formation yield upon the addition of an effective electron scavenger, such as $O_2$. This effect has been tentatively interpreted in terms of the following mechanism involving some ionic species for dimer production from the analogy of $Mo_2$ dimer:[29]

$$e^- + Cr(CO)_n \rightarrow Cr(CO)_{n-x}{}^- + x\,CO \qquad (0 \leq n \leq 6, 0 \leq x \leq n), \tag{1}$$

$$Cr^+ + Cr(CO)_{n-x}{}^- \rightarrow Cr_2{}^{(*)} + (n-x)CO. \tag{2}$$

Here, $Cr_2{}^{(*)}$ stands for a chromium dimer at an excited state or the ground state. The addition of an electron scavenger, such as $O_2$, decreases the dimer yield by suppressing the recombination processes, (1) and (2). Because the addition of an electron scavenger, such as $SF_6$, was reported to only little affect the de-

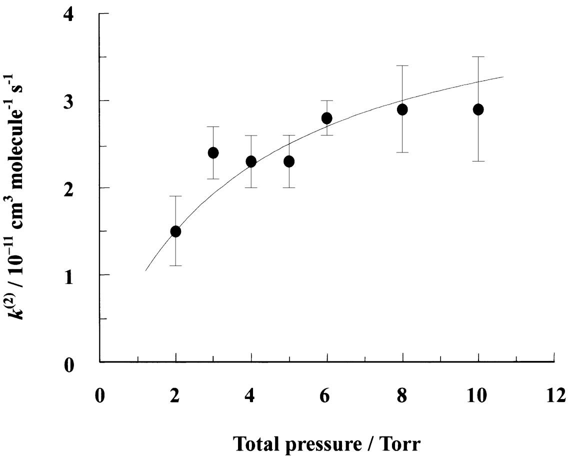

Fig. 4. Total pressure dependence of *pseudo*-second-order reaction rate constants ($k^{(2)}$) of $Cr_2$ (X $^1\Sigma_g{}^+$) with $O_2$. Total pressure is made to vary by change in Ar buffer gas pressure. Solid line is an empirical falloff curve fit (see text).

cay behavior of the $Mo_2$ dimer produced by the MPD of $Mo(CO)_6$, though the production yield of the metal dimer was affected by it,[24] only the decay part of the $Cr_2$ transient was analyzed by a least-square method to estimate the decay rate.

The dimer decay could be fitted by a single exponential function. In Fig. 3(a), the solid curves are the calculated ones for fitting in an appropriate time region. The decay rates of $Cr_2$ (X $^1\Sigma_g{}^+$, $v = 0$) were found to depend linearly on the $O_2$ pressure, as shown in Fig. 3(b), the slope of which gives a *pseudo*-second-order decay rate constant of $(2.3 \pm 0.3)\times10^{-11}$ cm$^3$ molecule$^{-1}$ s$^{-1}$ at a 6.0 Torr total pressure with balance Ar. Figure 4 shows the total pressure dependence of the *pseudo*-second-order decay rate constants, where the third body is Ar. Such a total pressure dependence is as expected from the simple Lindemann mechanism for an association reaction, as follows:

$$Cr_2 + O_2 \underset{k_{-1}}{\overset{k_1}{\rightleftarrows}} [Cr_2(O_2)]^* \xrightarrow{k_2[M]} Cr_2(O_2). \qquad (3)$$

In this mechanism, a *pseudo*-second-order rate constant is given as

$$k^{(2)} = \frac{k_1 k_2[M]}{k_{-1} + k_2[M]}. \qquad (4)$$

The solid line in the figure is a non-linear fitting curve, giving a $k_1$ of $(3.7 \pm 0.4)\times10^{-11}$ cm$^3$ molecule$^{-1}$ s$^{-1}$ and a $k_{-1}/k_2$ of $(7.3 \pm 2.4)\times10^{16}$ cm$^{-3}$ molecule. From these fitting results, the third-order rate constant of $Cr_2 + O_2 + Ar$ at the low-pressure limit is estimated to be $(5.9 \pm 2.5)\times10^{-28}$ cm$^6$ molecule$^{-2}$ s$^{-1}$. The $k_{-1}$ and $k_2$ rate constants could not be estimated individually from the data obtained in the limited total-pressure region. Based on the assumption that the collision diameter of $Cr_2O_2$ is $(6 \pm 1)$ Å, the collision frequency with Ar is estimated to be $(2.8 \pm 0.7)\times10^{-10}$ cm$^3$ molecule$^{-1}$ s$^{-1}$, which can be considered to be an upper limit for $k_2$; then, the upper limit for $k_{-1}$ is deduced to be about $(2.0 \pm 0.5)\times10^7$ s$^{-1}$ ($\tau \geq (50 \pm 10)$ ns). The collision diameter of $Cr_2O_2$ was roughly estimated by taking into account the bond lengths ($r(Cr_2) = 1.68$ Å,[10] $r(O_2) = 1.21$ Å,[30] and $r(CrO) = 1.62$ Å,[30]) and the expectation value of atomic orbital radii[31] ($\langle R\rangle_{3d}$ of Cr = 1.22 Å and $\langle R\rangle_{2p}$ of O = 1.23 Å). The existence of $Cr_2O_2$ was observed in a solid argon matrix by IR spectroscopy, which was expected to be a ring dimer.[32] A relatively long lifetime estimated by our kinetic analysis suggests that the association complex $Cr_2O_2$ has a loose structure with incidental weakened bond(s) other than the coordination bond. It seems possible for the $O_2$ molecule to be dissociatevely chemisorbed on the $Cr_2$ dimer only in the association process. An electron transfer from metal to the $\pi^*$-orbital of $O_2$ might explain the loose complex formation. The relatively low ionization potential reported for $Cr_2$ (6.999 eV)[33] is consistent with this association mechanism.

A similar kinetic measurement was carried out for Cr (a $^7S_3$) + $O_2$ at room temperature. In the limited total pressure region of 4–10 Torr with balance Ar, the *pseudo*-second-order rate constants depend almost linearly on the total pressure ($(1.0 \pm 0.4)\times10^{-11}$ cm$^3$ molecule$^{-1}$ s$^{-1}$ at 4 Torr, $(1.1 \pm 0.4)\times10^{-11}$ at 6 Torr, $(1.4 \pm 0.3)\times10^{-11}$ at 8 Torr, and $(1.7 \pm 0.3)\times10^{-11}$ at 10 Torr). A linear fitting of these data gave a slope value of $(4.1 \pm 0.7)\times10^{-29}$ cm$^6$ molecule$^{-2}$ s$^{-1}$. Parnis et al. measured the *pseudo*-second-order rate constants of Cr + $O_2$ over a wide total pressure region (2–600 Torr with Ar balance) and determined a third-order-rate constant of $(6.5 \pm 1.1)\times10^{-29}$ cm$^6$ molecule$^{-2}$ s$^{-1}$ from fitting the data to a simplified fall-off expression of Troe.[34] The fact that our value was small compared to their third-order rate constant suggests that a few Torr of total pressure with balance Ar was not sufficient to satisfy the low-pressure-limit condition. The mechanism of the reaction of the Cr atom with $O_2$ is suggested to be a two-step charge-transfer process (septet ($C_s$) → quintet ($C_{2v}$) → triplet ($C_{2v}$)) to form a triplet bent structure ($^3B_2$) by a DFT calculation.[19]

**b. $C_2H_4$ Addition.** Typical decay plots of $Cr_2$ in the presence of $C_2H_4$ at 6.0 Torr total pressure with balance Ar are presented in Fig. 5(a), where *pseudo*-first-order exponential decays were observed. The solid lines through data are single exponential decay fits from which the *pseudo*-first-order decay rates were estimated. The decay rates of $Cr_2$ plotted against the $C_2H_4$ pressure (Fig. 5(b)) were not influenced by $C_2H_4$ addition, while the primary $Cr_2$ yields slightly decreased with increasing the $C_2H_4$ pressure. The bimolecular rate constant of $Cr_2$ with $C_2H_4$ was estimated to be less than $4\times10^{-14}$ cm$^3$ molecule$^{-1}$ s$^{-1}$, meaning that $Cr_2$ was unreactive with $C_2H_4$ within the limit of our measurement.

The Cr atom was also observed to be unreactive with $C_2H_4$ at a total pressure of 6.0 Torr with balance Ar at room temperature ($k^{(2)} \leq 4\times10^{-14}$ cm$^3$ molecule$^{-1}$ s$^{-1}$), which is consistent with a previous observation.[34]

**c. $NH_3$ Addition.** Typical decay curves of $Cr_2$ (X $^1\Sigma_g{}^+$, $v = 0$) measured as a function of the $NH_3$ pressure are shown in Fig. 6(a). The total pressure was kept constant at 6.0 Torr using Ar as a balance gas. These *pseudo*-first-order decay rates increased proportionally with increasing the $NH_3$ pressure, giving a *pseudo*-second order rate constant of $(4.3 \pm 0.8)\times10^{-13}$ cm$^3$ molecule$^{-1}$ s$^{-1}$ (Fig. 6(b)). Within the total pressure region of 2.0–9.0 Torr with balance Ar, the *pseudo*-second-order rate constants were observed to be almost independent on the total pressure, as shown in Fig. 7. The average *pseudo*-second-order rate constant is $(4.2 \pm 0.6)\times10^{-13}$ cm$^3$

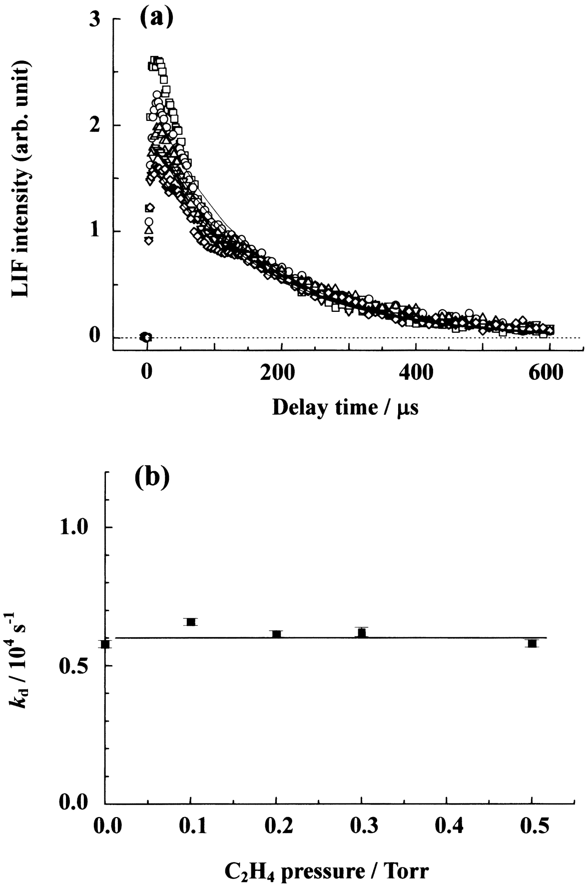

Fig. 5. (a) $C_2H_4$ addition effects on the transient LIF curves of $Cr_2$ (X $^1\Sigma_g{}^+$). $C_2H_4$ pressures are 0.0 (□), 0.1 (○), 0.2 (△), 0.3 (▽), and 0.5 Torr (◇); Each solid line is a single-exponential decay fit obtained with an appropriate decay rate. (b) $C_2H_4$ addition pressure dependence of the *pseudo*-first-order decay rates ($k_d$).

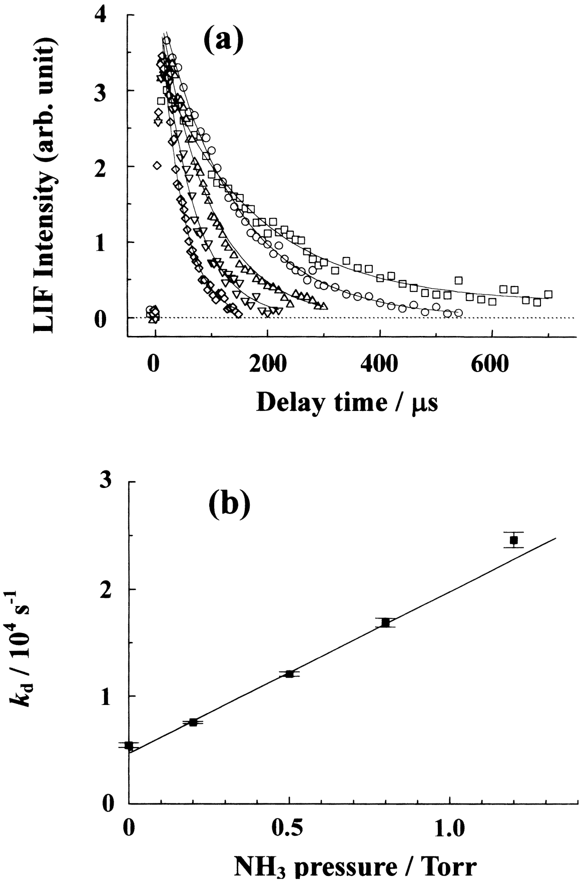

Fig. 6. (a) $NH_3$ addition effects on the transient LIF curves of $Cr_2$ (X $^1\Sigma_g{}^+$). $NH_3$ pressures are 0.0 (□), 0.2 (○), 0.5 (△), 0.8 (▽), and 1.2 Torr (◇); Each solid line is a single-exponential decay fit obtained with an appropriated decay rate. (b) $NH_3$ addition pressure dependence of the *pseudo*-first-order decay rates ($k_d$); Solid line is only an average line.

molecule$^{-1}$ s$^{-1}$, which is considered to be a second-order rate constants at the high-pressure limit at room temperature.

The Cr atom was observed to be unreactive with $NH_3$ at a total pressure of 6.0 Torr with balance Ar at room temperature ($k^{(2)} \leq 4\times10^{-14}$ cm$^3$ molecule$^{-1}$ s$^{-1}$).

**d. Comparison of the Reactivity of Transition-Metal Dimers.** The rate constants estimated from our experiment are summarized in Table 1 together with the previously reported values. The tendency observed in the reactivity of $Cr_2$, which reacts with $NH_3$ (σ-acceptor), but not with $C_2H_4$ (π-donor), is consistent with that of $Mo_2$ belonging to the same group VI. Both metal dimers are reactive to the oxygen molecule, which is in contrast with the coinage metal dimers.

A quasi-linear structure is expected for the [$Mo_2(NH_3)$] complex, because its bonding interaction is a σ-donation from the nitrogen lone pair of $NH_3$ to the lowest unoccupied orbital (one of sp hybrids of Mo) of $Mo_2$.[17] This interaction seems to extrapolate to the [$Cr_2(NH_3)$] complex as well as the coinage dimer complex. The sextuply bonded leading configuration is thought to comprise only 61% of the total wave function by a MCSCF with a CI calculation.[36] The dominant excited configurations in the CI wave function are the result of excitation from the $2\delta_g$ orbital to the $2\delta_u$ orbital. This open signet character may be the origin of the assumed large polarizability to accept the lone-pair electron of $NH_3$, and also of the radical-radical interaction with $O_2$ of the group-VI metal dimers. The ionization potentials of coinage dimers (*IP*($Cu_2$) = 7.894 eV, *IP*($Ag_2$) = 7.56 eV)[9] are fairly higher than those of group-VI metal dimers (*IP*($Cr_2$) = 6.999 eV, *IP*($Mo_2$) = 6.948 eV).[33] The apparent discrepancy between these two groups in the reactivity with $O_2$ may also support that there is an electron-transfer process from metal to $O_2$ ($\pi^*$-orbital) in the early stage.

## Conclusions

The MPD of [$Cr(CO)_6$] has been applied to the pulse production of "naked" $Cr_2$ dimers in the gas phase for neutral gas kinetic studies. The tendency in reactivity for $Cr_2$ obtained from the time-resolved measurement was substantially consistent with the observation for $Mo_2$ using laser vaporization/LIF in a flow tube,[17] in which a group-VI transition metal dimer reacts with $NH_3$ (σ-acceptor), but not with $C_2H_4$ (π-donor). In order to elucidate the intricate interaction between the transition-metal species and the ligands, systematic measurements

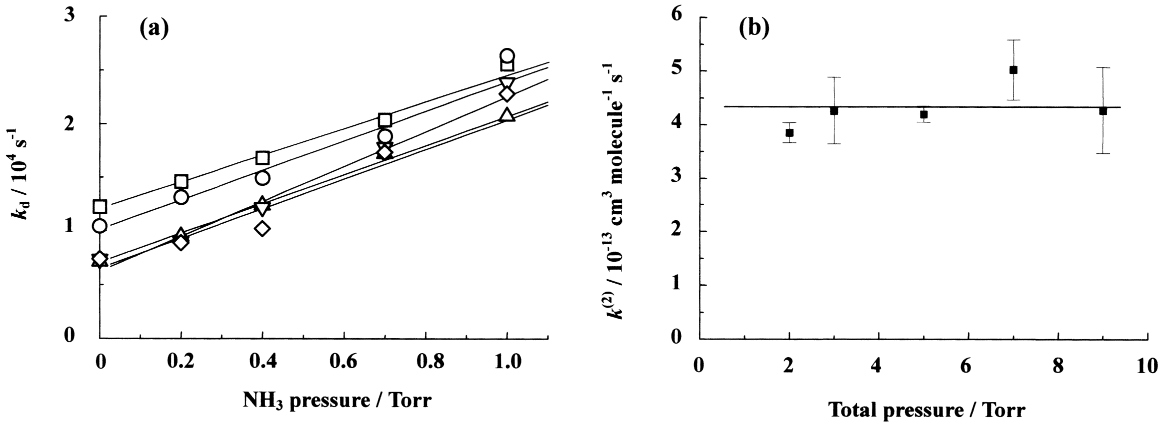

Fig. 7. (a) Total pressure effects on the *pseudo*-first-order decay rates ($k_d$) of $Cr_2$ ($X\ ^1\Sigma_g^+$) in the presence of $NH_3$. Total pressures are 2.0 (□), 3.0 (○), 5.0 (△), 7.0 (▽), and 9.0 Torr (◇); Each solid line is a linear fit. Total pressure is made to vary by change in Ar buffer gas pressure. (b) Total pressure dependence of *pseudo*-second-order reaction rate constants ($k^{(2)}$) of $Cr_2$ ($X\ ^1\Sigma_g^+$) with $NH_3$. Solid line is only an average line.

Table 1. Reaction Rate Constants for Transition Metal Dimers with $O_2$, $C_2H_4$, and $NH_3$ at Room Temperature[a, b)]

| Reactant | $Cr_2$ ($X\ ^1\Sigma_g^+$) | $Mo_2$ ($X\ ^1\Sigma_g^+$) | $Cu_2$ ($X\ ^1\Sigma_g^+$) | $Ag_2$ ($X\ ^1\Sigma_g^+$) | $Au_2$ ($X\ ^1\Sigma_g^+$) |
|---|---|---|---|---|---|
| $O_2$ | $k^{(2)}$;<br>$(2.3 \pm 0.3)\times10^{-11}$<br>(Ar; 6.0)<br>$k^{(3)}$;<br>$(5.9 \pm 2.5)\times10^{-28}$<br>(M = Ar)<br>$k_\infty$;<br>$(3.7 \pm 0.4)\times10^{-11}$ | $k^{(2)}$;<br>$1.0\times10^{-11}$<br>(He; 0.45−2.3)[17]<br>$(1.1 \pm 0.1)\times10^{-11}$<br>(Ar; 6.5)[35] | NR[16] | NR[16] | NR[16] |
| $C_2H_4$ | NR (Ar; 6.0) | NR (He; 8)[17]<br>NR (Ar 6.5)[24] | $k^{(3)}$;<br>$(9.3 \pm 1.4)\times10^{-30}$<br>(M = He)[15] | NR[16] | $k^{(3)}$;<br>$(2.3 \pm 0.5)\times10^{-28}$<br>(M = He)[16] |
| $NH_3$ | $k^{(2)}$;<br>$(4.3 \pm 0.8)\times10^{-13}$<br>(Ar; 6.0)<br>$k_\infty$;<br>$(4.2 \pm 0.6)\times10^{-13}$ | $k^{(2)}$;<br>$2.5\times10^{-13}$<br>(He; 7.8)[17]<br>$(9 \pm 2)\times10^{-13}$<br>(Ar; 6.5)[24] | $k^{(3)}$;<br>$(8.8 \pm 1.2)\times10^{-30}$<br>(M = He)[16] | $k^{(3)}$;<br>$(1.0 \pm 0.3)\times10^{-30}$<br>(M = He)[16] | $k^{(3)}$;<br>$(2.2 \pm 0.4)\times10^{-29}$<br>(M = He)[16] |

a) $k^{(2)}$, *pseudo*-second-order rate constant/cm$^3$ molecule$^{-1}$ s$^{-1}$: $k^{(3)}$, third-order rate constant at the low pressure limit/cm$^6$ molecule$^{-2}$ s$^{-1}$; M, third body: $k_\infty$, second-order rate constant at the high pressure limit/cm$^3$ molecule$^{-1}$ s$^{-1}$.
b) Total pressure or range (unit, Torr) are shown in parentheses together with balance gas.

would be required over a wider total pressure and temperature range.

## References

1 "Gas Phase Inorganic Chemistry," ed by D. H. Russell, Plenum Press, New York (1989).

2 "Bimolecular Collisions," ed by M. N. R. Ashfold and J. E. Baggott, Royal Society of Chemistry, London (1989).

3 "Laser Chemistry of Organometallics,"ACS Symposium Series, ed by J. Chaiken, 530 (1993).

4 Y. Wen, A. Yethirai, and J. C. Weisshaar, *J. Chem. Phys.*, **106**, 5509 (1997).

5 M. L. Campbell, *J. Phys. Chem. A*, **102**, 892 (1998).

6 K. Honma, *J. Phys. Chem. A*, **103**, 1809 (1999).

7 "Quantum Chemistry: The Challenge of Transition Metals and Coordination Chemistry," NATO ASI Series C, ed by A. Veillard (1986), Vol. 176.

8 "Metal-Ligand Interactions in Chemistry, Physics and Biology," NATO Science Series C, ed by N. Russo and D. R. Salahub (2000), Vol. 546.

9 M. D. Morse, *Chem. Rev.*, **86**, 1049 (1986).

10 D. R. Salahub, in "Ab Initio Methods in Quantum Chemistry II," ed by K. P. Lawley, John Wiley & Sons Ltd., New York, (1987) p. 447.

11 M. D. Morse, M. E. Geusic, J. R. Heath, and R. E. Smalley,

*J. Chem. Phys.*, **83**, 2293 (1985).

12 D. M. Cox, K. C. Reichmann, D. J. Trevor, and A. Kaldor, *J. Chem. Phys.*, **88**, 111 (1988).

13 S. A. Mitchell, L. Lian, D. M. Rayner, and P. A. Hackett, *J. Chem. Phys.*, **103**, 5539 (1995).

14 S. A. Mitchell, D. M. Rayner, T. Bartlett, and P. A. Hackett, *J. Chem. Phys.*, **104**, 4012 (1996).

15 L. Lian, F. Akhtar, P. A. Hackett, and D. M.Rayner, *Chem. Phys. Lett.*, **205**, 487 (1993).

16 L. Lian, P. A. Hackett, and D. M. Rayner, *J. Chem. Phys.*, **99**, 2583 (1993).

17 L. Lian, S. A. Mitchell, and D. M. Rayner, *J. Phys. Chem.*, **98**, 11637 (1994).

18 H. Nakatsuji, M. Hada, and T. Yonezawa, *J. Am. Chem. Soc.*, **109**, 1902 (1987).

19 A. Martínez, *J. Phys. Chem. A*, **102**, 1381 (1998).

20 A. Martínez, C. Jamorski, G. Medina, and D. R. Salahub, *J. Phys. Chem. A*, **102**, 4643 (1998).

21 Y. M. Efremov, A. N. Samoilova, and L. V. Gurvich, *Opt. Spectrosc.*, **36**, 381 (1974).

22 Y. M. Efremov, A. N. Samoilova, V. B. Kozhukhovsky, and L. V. Gurvich, *J. Mol. Spectrosc.*, **73**, 430 (1978).

23 S. A. Mitchell and P. A. Hackett, *J. Chem. Phys.*, **93**, 7822 (1990).

24 Y. Ishikawa, Y. Matsumoto, and T. Wakabayashi, *Bull. Chem Soc. Jpn.*, **72**, 2633 (1999).

25 S. J. Riley, E. K. Parks, L. G. Pobo, and S. Wexler, *J. Chem. Phys.*, **15**, 2577 (1983).

26 V. E. Bondybey and J. H. English, *Chem. Phys. Lett.*, **94**, 443 (1983).

27 D. L. Mlchalopoulos, M. E. Geusic, S. G. Hansen, D. E. Powers, and R. E. Smalley, *J. Phys. Chem.*, **86**, 3914 (1982).

28 "Atomic Energy Levels, Vol. II," NSRDS-NBS 35, ed by C. E. Moore (1971).

29 Y. Nakai, T. Wakabayashi, and Y. Ishikawa, *Appl. Phys. B*, **66**, 621 (1998).

30 "Constants of Diatomic Molecules," ed by K. P. Huber and G. Herzberg, Van Nostrand Reinhold Company, New York (1979).

31 "The Hartree-Fock Method for atoms," ed by C. H. Fischer, John Wiley & Sons, New York (1977).

32 G. V. Chertihin, W. D. Bare, and L. Andrews, *J. Chem. Phys.*, **107**, 2798 (1997).

33 B. Simard, M.-A. Lebeault-Dorget, A.Marijnissen, and J. J. ter Meulen, *J. Chem. Phys.*, **108**, 9668 (1998).

34 J. M. Parnis, S. A. Mitchell, and P. A. Hackett, *J. Phys. Chem.*, **94**, 8152 (1990).

35 T. Wakabayashi, Y. Ishikawa, and S. Arai, *Chem. Phys. Lett.*, **256**, 543 (1996).

36 B. E. Bursten, F. A. Cotton, and M. B. Hall, *J. Am. Chem. Soc.*, **102**, 6349 (1980).